Tailoring chemotherapy for the African-centric S47 variant of TP53

Thibaut Barnoud[1], Anna Budina-Kolomets[1], Subhasree Basu[1], Julia I-Ju Leu[2], Madeline Good[1], Che-Pei Kung[3], Jingjing Liu[1], Qin Liu[1], Jessie Villanueva[1], Rugang Zhang[4], Donna L. George[2] and Maureen E. Murphy[1*]

[1]Program in Molecular and Cellular Oncogenesis, The Wistar Institute, Philadelphia PA 19104, USA, [2]Department of Genetics, The Perelman School of Medicine at the University of Pennsylvania, Philadelphia, PA 19104, USA, [3]ICCE Institute and Department of Internal Medicine, Division of Molecular Oncology, Siteman Cancer Center, Washington University School of Medicine, St Louis MO 63110, USA, [4]Gene Expression and Regulation Program, The Wistar Institute, Philadelphia PA 19104, USA

The authors declare no potential conflicts of interest.

Running Title: Cisplatin and BET inhibitors Suppress *TP53* Pro47Ser Tumors

Key Words: p53, Pro47Ser, Cisplatin, BET inhibitors, mitochondria

*Correspondence:

Maureen Murphy, Ph.D.

Professor and Program Leader, Molecular and Cellular Oncogenesis Program

The Wistar Institute

3601 Spruce Street, Room 356

Philadelphia, PA 19104

Phone: (215) 495-6870

email: mmurphy@wistar.org

ABSTRACT

The tumor suppressor *TP53* is the most frequently mutated gene in human cancer and serves to restrict tumor initiation and progression. Single nucleotide polymorphisms (SNPs) in *TP53* and p53 pathway genes can have a marked impact on p53 tumor suppressor function, and some have been associated with increased cancer risk and impaired response to therapy. Approximately 6% of Africans and 1% of African-Americans express a p53 allele with a serine instead of proline at position 47 (Pro47Ser). This SNP impairs p53-mediated apoptosis in response to radiation and genotoxic agents and is associated with increased cancer risk in humans and in a mouse model. In this study, we compared the ability of wild type (WT) and S47 p53 to suppress tumor development and respond to therapy. Our goal was to find therapeutic compounds that are more, not less, efficacious in S47 tumors. We identified the superior efficacy of two agents, cisplatin and BET inhibitors, on S47 tumors compared to WT. Cisplatin caused dramatic decreases in the progression of S47 tumors by activating the p53/PIN1 axis to drive the mitochondrial cell death program. These findings serve as important proof of principle that chemotherapy can be tailored to p53 genotype.

Significance: A rare African-derived, radio-resistant p53 SNP provides proof of principle that chemotherapy can be tailored to TP53 genotype.

INTRODUCTION

The p53 tumor suppressor acts as a central signaling hub in response to oncogenic, genotoxic and metabolic stress (1-3). In turn, p53 inhibits tumorigenesis by engaging numerous pathways, including cell cycle arrest, apoptosis, senescence, and ferroptosis (4-6). It is also a key determinant of the efficacy of numerous chemotherapeutic compounds (7,8). Whereas most p53 pathways require the ability of this protein to function as a transcription factor, the apoptotic pathway by p53 also possesses a transcription-independent, direct mitochondrial role (9-11). Mutations in p53 in human tumors abrogate all of these tumor suppressive pathways, and render tumors poorly responsive to therapy. In addition, in tumors with wild type (WT) p53 there is strong evidence that single nucleotide polymorphisms in TP53 and p53 pathway genes can decrease tumor suppression, as well as the response to cancer therapy.

A nonsynonymous single-nucleotide polymorphism at codon 47 in *TP53* was reported over twenty years ago in African-descent populations and that has now been implicated in cancer (12). Approximately 6% of Africans and 1% of African-Americans express a p53 allele with a serine residue at codon 47 (Pro47Ser, rs1800371). We created a mouse model for this variant, hereafter S47, and showed that mice expressing this variant in either heterozygous or homozygous form show increased risk for hepatocellular carcinoma and other cancers (13). We also showed that this variant of p53 demonstrates reduced phosphorylation on serine 46, as well as decreased ability to induce cell death by radiation and genotoxic stress (13,14). These findings led to the possibility that individuals with the S47 variant might show reduced efficacy of cancer therapy. To test this hypothesis, we created transformed versions of WT and S47 cells using mouse embryonic fibroblasts from

the WT and S47 mouse, following infection with the adenoviral E1A oncogene and activated RAS. Our goal was to use these reagents to determine whether S47 tumor cells showed enhanced tumorigenic properties, along with decreased sensitivity to commonly used chemotherapeutic drugs. We also sought to use these reagents to test the possibility that drugs might be discovered that preferentially targeted the S47 variant of p53. This might likewise reveal cell death pathways exploitable in S47 tumors. Here-in we show that this paradigm has been successful, and we have identified two chemotherapeutic compounds that are preferentially cytotoxic to S47 tumors, compared to WT p53. These studies serve as important proof of principle that chemotherapy can be tailored to p53 genotype, and they have important implications for individuals of African descent who are afflicted with cancer.

MATERIALS AND METHODS

Cell Lines and Culture Conditions

Wild type (WT) and S47 primary MEFs and E1A/RAS transformed clones were generated previously, and MYC/RAS clones were generated as described (15). E1A/RAS MEFs and H1299 lung adenocarcinoma cells were grown in DMEM (Corning Cellgro™, Corning, NY, USA) supplemented with 10% Fetal Bovine Serum (HyClone™, GE Healthcare Life Sciences) and 1% penicillin/streptomycin (Corning Cellgro™). WM278 cells were maintained in 80% MCDB153 (Sigma Aldrich, St. Louis, MO, USA)/ 20% Liebovitz L-15 (Corning Cellgro™) media supplemented with 2% FBS and 1.68 mM $CaCl_2$. Cell line authentication used STR profiling (ATCC). Cells were grown in a 5% CO_2 humidified incubator at 37°C. Cell lines were tested for mycoplasma every six months. Cell viability, clonogenic survival and soft agar assays were done as described (13,16,17).

Antibodies and Reagents

Antibodies used were: p53 (2524S), Cleaved Caspase-3 (9661S), Cleaved Lamin A (2035S), Histone H3 (3638T), HSP90 (4877S), BAK (12105S), Ki-67 (12202S), PIN1 (3722S), c-MYC (5605S) and GAPDH (2118S) (Cell Signaling, Danvers, MA, USA), RAS (610001), Cytochrome C (556433) (BD Biosciences, Franklin Lakes, NJ, USA), p21 (ab109199) and BRD4 (ab128874, Abcam, Cambridge, MA, USA), BRD2 (A302-583A, Bethyl Laboratories, Montgomery, TX, USA), H3 pan-Ac (39139, Active Motif, Carlsbad, CA, USA), PCNA (sc-56), PIN1 (sc-15340), p53 (FL-393, sc-6243) and TOMM20 (sc-11415) (Santa Cruz Biotechnology, Dallas, TX, USA), and BAK-NT (06-536, MilliporeSigma, Burlington, MA, USA). Chemotherapeutic compounds were: Etoposide (E1383, Sigma Aldrich), Cisplatin (HY-17394) and OTX-015 (HY-15743) (MedChem Express, Monmouth Junction, NJ, USA),

JQ-1 (11187), I-BET151 (11181), I-BET762 (10676), and Carboplatin (13112, Cayman Chemical, Ann Arbor, MI, USA), and Nedaplatin (S1826, Selleck Chemicals, Houston, TX, USA). For in vitro studies, OTX-015 was dissolved in DMSO (D8418, Sigma Aldrich). For in vivo studies, a stock of 100 mg/mL OTX-015 in DMSO was dissolved in 10% 2-Hydroxypropyl-beta-cyclodextrin (HP-β-CD) (CTD Holdings, Alachua, FL) in sterile water to give a final DMSO concentration of 6.25% (v/v). All compounds were dissolved in 0.9% saline solution (Sigma Aldrich, S8776). PIN1 SMARTPool siRNA was from Dharmacon (Lafayette CO USA).

Mitochondria Isolation, BAK Oligomerization Assays, Immunoblotting

The full-length human p53 (residues 1-393) and human p53 (residues 2-393) were cloned into the pET25 vector (MilliporeSigma, Burlington, MA, USA) and the pGEX-4T-3 vector (GE Healthcare Life Sciences, Chicago, IL, USA) respectively. Recombinant GST-tagged p53 proteins and N-terminal His_6-tag-p53 proteins were purified using protocols from the manufacturer and purified proteins were dialyzed against Assay Buffer (10 mM Hepes/KOH, pH 7.4, 5 mM KH_2PO_4, 5 mM Succinate, and 250 mM Sucrose) at 4°C. In vitro BAK oligomerization assays were performed as described previously (11,18). Briefly, 25 µg of purified mitochondria were incubated with 100 pmol of recombinant p53 proteins. After 30 min incubation at 4˚C, the BAK oligomers were crosslinked with freshly-made 2.8 mM bismaleimidohexane (BMH) (Thermo Fisher Scientific) for 30 min at 30˚C, prior to the addition of SDS loading buffer. Oligomerization products were size fractionated on 4-20% Tris-Glycine gradient gels (Lonza, Walkersville, MD, USA) and subjected to Western blotting using the BAK specific antibody anti-BAK-NT (Millipore Sigma). For all other Western blot analysis, 50-100 µg of whole-cell lysate was resolved over SDS PAGE gels using pre-cast

10% NuPAGE Bis-Tris gels (Thermo Fisher Scientific) and transferred onto PVDF membranes (IPVH00010, pore size: 0.45 μm) (Millipore Sigma) prior to analysis.

Proximity Ligation Assays

PLA was performed as described previously (19). Briefly, E1A/RAS cells were grown on Lab-Tek II 8-well chamber slides and fixed for endogenous protein detection as described above, using the Duolink kit (Sigma Aldrich). As a negative control, one of the primary antibodies was omitted. For in vivo PLA, the Duolink PLA Brightfield kit (Sigma Aldrich) was used according to the manufacturer's protocol. Quantification of PLA signals was performed using ImageJ Software (NIH, Rockville, MD, USA).

Tumor studies

All studies were carried out in accordance with the recommendations in the Guide for the Care and Use of Laboratory Animals of the National Institutes of Health (NIH). All protocols were approved by The Wistar Institute Institutional Animal Care and Use Committee (IACUC). Both male and female mice were used, between 6 and 10 weeks of age. Mice were housed in plastic cages with ad libitum diet and maintained with a 12-h dark/12-h light cycle at 22°C. For tumor growth experiments, WT or S47 E1A/RAS MEFs were injected subcutaneously into the right flanks of 8-week old male or female NSG (NOD.Cg-Prkdcscid Il2rgtm1Wjl/SzJ) mice. Tumor volumes were measured using digital calipers and tumor volume was calculated using the formula: volume = (length x width^2) x 0.52. All mice were monitored daily for signs of pain or distress. When tumors reached 10% of body weight, mice were euthanized. Immunohistochemistry of formalin-fixed tissues was performed as previously described (20).

For lung colonization studies, 5 x 10^5 cells from WT or S47 E1A/RAS MEFs were injected into the tail vein of 8-week old NSG mice. Mice were monitored daily for two weeks; at day 14 mice were euthanized, and the lungs were formalin fixed for further analysis. For therapy experiments, WT and S47 E1A/RAS MEFs were sub-cutaneously injected into 6-8 week old NSG mice as described above. Once mice obtained palpable tumors (approximately 100 mm^3) mice were randomly assigned into separate groups (8 mice per group): dilution vehicle, cisplatin, etoposide, or OTX-015. Cisplatin and etoposide were administered at a concentration of 4 mg/kg and 10 mg/kg, respectively, by intra-peritoneal injection every four days. OTX-015 was administered daily by oral gavage at a concentration of 50 mg/kg. Tumor volumes were measured every other day until the control groups contained tumors that were 10% of body weight, at which point all mice were euthanized.

Statistical analysis of data

Unless otherwise stated all experiments were carried out in triplicate (n=3) on both independent clones of E1A/RAS MEFs of each genotype (WT and S47). All mouse experiments had a minimum of n=8 per experimental group. For in vitro studies, the two-tailed unpaired Student t-test was performed. All in vitro data are reported as the mean ± standard deviation unless stated otherwise, and in vivo data are reported as the mean ± standard error. The tumor volume data are longitudinal; because the growth trends are observed in piecewise linear manner during the follow-up period, we applied a mixed effects model with linear spline regression to estimate and compare the tumor growth velocities between experimental groups, as described previously (21,22). Statistical analyses were

performed using GraphPad Prism. p values are as indicated: * = $p<0.05$, ** = $p<0.01$, and *** $p < 0.001$.

RESULTS

The S47 variant is an intrinsically poorer tumor suppressor

Our data in a mouse model indicated that the S47 mouse was markedly susceptible to hepatocellular cancer and histiocytic sarcoma (13). However, the possibility remained that the S47 variant was an intrinsically poorer tumor suppressor compared to WT p53 in other tissues and cell types as well. To address this question, we generated WT and S47 transformed cells using mouse embryonic fibroblasts (MEFs) that were retrovirally infected and transformed with the oncogenes E1A and RAS **(Supp. Fig. 1A)**. To ensure reproducibility we generated two clones of each and analyzed and pooled all data from both clones for each experiment described here-in. We sequenced the entire p53 coding region from these clones and ensured there were no second-site mutations.

We tested our WT and S47 E1A/RAS cell lines for several markers of transformation, including growth in low serum, growth in soft agar, and growth as xenograft tumors. While WT and S47 transformed cells proliferated similarly in normal culture conditions, WT cells were growth inhibited in low serum; in contrast S47 cells continued proliferating (**Fig. 1A and B**). Both WT and S47 clones showed equivalent numbers of colonies in soft agar, but we noted a consistent increase in colony size for the transformed S47 clones (**Fig. 1C and D**). Notably, we found a consistently increased ability of S47 transformed cells to develop as xenograft tumors, compared to the WT clones; this was reflected in more rapid kinetics of growth and increased S47 tumor weights at the conclusion of the study (**Fig. 1E and F**). Immunohistochemical analysis of WT and S47 xenograft tumors of approximately similar size revealed equivalent p53 staining but markedly increased Ki-67 staining in S47 tumors (**Fig. 1G**).

We next sought to test the possibility that S47 might be a poorer suppressor of lung colonization in a tail vein assay, relative to WT p53. This question was of interest because a fraction of S47 knock-in mice develop tumor metastases (13). Toward this goal we injected equal numbers of WT and S47 E1A/RAS cells into the tail vein of immunocompromised mice. Two weeks following injection, we assessed lung histology and metastatic burden, and found significantly increased lung weights and tumor burden for S47 cells (**Supp. Fig. 1B and C**), as well as increased Ki-67 immunostaining in S47 tumors (**Supp. Fig. 1D**) and tumor burden (**Supp. Fig 1E**). The combined data indicate that the S47 protein is an intrinsically poorer tumor suppressor compared to WT p53, at least for the oncogene combinations and assays used here.

Transformed S47 cells show increased sensitivity to cisplatin

We previously showed that non-transformed S47 cells are resistant to conventional agents of genotoxic stress, including adriamycin and etoposide (13). In contrast, we found that transformed S47 tumor cells show increased sensitivity to cisplatin in vitro, compared to WT p53 (15). The increased sensitivity of transformed S47 cells held true for multiple concentrations of cisplatin (**Fig. 2A**) and was consistent when tumor cells were grown in soft agar (**Fig. 2B, C**). This increased sensitivity of transformed S47 cells was also evident for other platinum-based compounds, like nedaplatin and carboplatin (**Fig. 2D**). We next transformed WT and S47 cells with another oncogene combination, MYC plus oncogenic RAS. These transformed S47 cells showed 2.5-fold enhanced sensitivity to cisplatin compared to WT p53 (**Supp. Fig. 2A and B**). It is important to note that primary S47 MEFs do not show increased sensitivity to cisplatin, in fact they are resistant to this drug (13), so this is a property only of transformed S47 cells. Finally, we used CRISPR/Cas9 gene editing to convert the WT p53 in the WM278 (BRAF V600E mutant) melanoma cell line to S47; we

chose this cell line because it is homozygous for the proline 72 variant of p53, which is the relevant background upon which the S47 SNP arose (14). We generated two S47 knock-in clones, one with a heterozygous knock-in (WT/S47) and one with a homozygous knock-in (S47/S47). Because the S47/S47 clone showed markedly reduced steady state levels of p53 protein, we chose to focus on the WT/S47 line. Despite showing slightly reduced level of p53 protein compared to the parental clone, the WT/S47 line showed markedly increased cell death following cisplatin treatment (**Supp. Fig. 2C**). These WT/S47 cells also showed reduced IC50, compared to control cells, to cisplatin, nedaplatin and carboplatin (**Supp. Fig. 2D**). The combined data are consistent with the premise that the S47 variant confers increased sensitivity to platinum-based compounds, independent of tumor background.

Transformed S47 cells show increased sensitivity to BET inhibitors

Our findings with cisplatin were proof of principle that drugs could be discovered that could effectively treat tumors containing the S47 variant. Therefore, we next performed a cell viability screen of a library of over 200 conventional and experimental chemotherapeutic drugs, using our WT and S47 E1A/RAS clones. The majority of tested compounds showed either reduced efficacy in S47 transformed cells, or no differences in drug sensitivity between WT and S47 transformed lines. Notably however, a small subset of epigenetic compounds showed increased sensitivity in S47 cells: these were from the class of BET protein (bromo-domain and extra-terminal motif) inhibitors **(Supp. Table 1)**. Analysis of cell viability of WT and S47 cells treated with several BET protein inhibitors, including the well-characterized tool compound JQ-1 (23) and the BRD2/4 inhibitor OTX-015 (currently in clinical trials (24,25)) revealed that S47 cells show a 4 to 5-fold increased sensitivity to BET inhibitors, compared to tumor cells with WT p53 (**Fig. 2E and Supp. Fig. 2E)**. In contrast, there was no difference in cell viability in response to the broad-spectrum bromodomain inhibitor bromosporine **(Supp.**

Table 1). Clonogenic survival assays with WT and S47 E1A/RAS MEFs and the BET inhibitor OTX-015 confirmed that S47 transformed cells showed significantly reduced colony forming ability following treatment with OTX-015 compared to WT p53 (**Fig. 2F and G)**.

Cisplatin and OTX-015 show superior ability to suppress the growth of S47 tumors

We next sought to test the efficacy of cisplatin and BET inhibitors against WT and S47 tumors in vivo. Toward this goal we injected equal numbers of both clones of WT and S47 E1A/RAS MEFs subcutaneously into immunocompromised mice. Once tumors reached 100 mm^3, mice were randomized and treated by daily oral gavage with OTX-015 or by intra-peritoneal injections every four days with 4 mg/kg cisplatin. As expected, untreated S47 tumors grew significantly faster than WT tumors (**Fig. 3A**). Notably however, both OTX-015 and to a greater extent cisplatin showed markedly increased ability to cause tumor regression of S47 tumors compared to WT (**Fig. 3A and B**). We realized that the increased proliferative rate of S47 tumors relative to WT might contribute to the increased efficacy of these drugs in S47 tumors. Therefore, we repeated this study using another genotoxic agent, etoposide, which does not show preferential toxicity in S47 transformed cells in vitro. Unlike OTX-015 and cisplatin, etoposide did not show evidence for increased efficacy in S47 tumors compared to WT (**Fig. 3C and D)**. We analyzed the kinetics of tumor regression following treatment using a spline mixed model; this analysis assesses the reduction in tumor volume per measurement window. A spline mixed model analysis confirmed that cisplatin, and to a lesser extent OTX-015, led to significantly greater decreases in tumor volume per treatment window in S47 compared to WT tumors ($p<0.0001$ between S47 and WT for cisplatin; $p=0.0058$ between S47 and WT for OTX-015) (**Fig. 3E and F**). In contrast, the efficacy of etoposide between WT and S47 did not show statistically significant differences (**Fig. 3G**). Immunohistochemical analysis of cisplatin-treated WT and S47 tumors revealed that this

treatment led to decreased Ki-67 immunostaining in both WT and S47 tumors. In addition, in S47 tumors there was a significant increase in staining for cleaved caspase-3 compared to WT (**Fig. 3H**). These data suggested that the increased efficacy of cisplatin in S47 tumors was caused by increased apoptosis.

We next sought to identify potential underlying mechanisms for increased sensitivity of S47 tumors to cisplatin and BET inhibitors. BET inhibitors like JQ-1 and OTX-015 bind to the BET proteins BRD2, -3 and -4, and prevent these proteins from binding to chromatin; in some cases, BET inhibitors also cause down-regulation of BET proteins (26). In some cases, the cytotoxicity of BET inhibitors can be correlated with their ability to cause down-regulation of the MYC oncoprotein (27,28). We treated WT and S47 E1A/RAS cells with JQ1 or OTX-015 and monitored the level of BRD-2 and -4, as well as MYC. We found that there were no differences in the level of BRD-2 and -4 in untreated WT and S47 cells, and that JQ-1 and OTX-015 caused a modest down-regulation of BRD2 in S47 transformed cells, but no change in BRD4 level **(Supp. Fig. 2F)**. In contrast, we found that OTX-015 led to a marked down-regulation of MYC in E1A/RAS-S47 transformed cells, much greater than that in WT cells **(Supp. Fig. 2G)**. This profound decrease in c-MYC might be a cause for the increased cytotoxicity of OTX-015 in S47 cells. Interestingly, we also saw a marked down-regulation of MYC in E1A/RAS S47 cells treated with cisplatin (**Supp. Fig. 2H**), suggesting a potentially broad role for MYC in cisplatin sensitivity; this is consistent with the findings of others (29). We also observed increased acetylated histone H3 in S47 cells, which may explain increased sensitivity to BET inhibitors (**Supp. Fig. 2I**). Because our data indicated that cisplatin outperformed BET inhibitors in S47 tumors, we focused further on understanding the mechanistic basis for increased sensitivity to cisplatin.

Enhanced transcription-independent apoptosis in S47 transformed cells following cisplatin treatment

To begin to elucidate the potential mechanism for enhanced cell death of S47 cells by cisplatin, we first assessed the transcriptional pathway of p53-mediated cell death and performed QPCR of a dozen p53 target genes; we did not see increases in the pro-apoptotic genes PUMA, NOXA and BAX in S47 transformed cells, compared to WT, following cisplatin treatment. Therefore, we next sought to assess the transcription-independent cell death pathway of p53, which uses a direct mitochondrial mechanism of cell death involving a direct interaction of p53 with BCL2 family members (9-11). To do this, we first tested the ability of cycloheximide (CHX), which blocks the transcriptional pathway by inhibiting new protein synthesis (30), to block cisplatin-mediated apoptosis. We also purified mitochondria from WT and S47 E1A/RAS cells, and used western blotting to assess the level of p53 co-localized with this organelle. Finally, we performed proximity ligation assays (PLA) to assess the p53-BAK interaction, which is important in transcription-independent apoptosis (12). We found that CHX treatment inhibited the induction of the p53-target protein p21 (CDKN1A), but had no effect on apoptosis in S47 cells, as assessed by the accumulation of cleaved caspase-3 (**Fig. 4A, compare CC3 lanes 6 and 8**). We next isolated purified mitochondria from untreated and cisplatin-treated WT and S47 E1A/RAS cells, and found markedly increased amount of the S47 protein at the mitochondria of treated cells, compared to WT p53 (arrows, **Fig. 4B)**. Consistent with this, PLA analysis revealed increased association of S47 protein with BAK at the mitochondria of S47 cells following cisplatin treatment, compared to WT cells (**Supp. Fig. 3A**). These combined findings support the conclusion that the increased cell death of transformed S47 cells by cisplatin is through increased usage of the direct mitochondrial, transcription-independent cell death pathway of p53.

The peptidyl-prolyl isomerase PIN1 interacts directly with p53 and is required for the localization of p53 to mitochondria (31). Although serine 46 phosphorylation is important for the PIN1 interaction, there are many PIN1-binding sites in p53 protein (32). To determine whether PIN1 plays a role in the increased trafficking of S47 to the mitochondria following cisplatin treatment, we performed PLA to assess the interaction of WT p53 and S47 with PIN1. PLA analyses showed that the association between S47 and PIN1 was markedly increased, compared to WT p53 (**Fig. 4C**), while there were equivalent levels and immunostaining of p53 and PIN1 in WT and S47 cells (**Supp. Fig. 3B**). We next silenced PIN1 using siRNA in WT and S47 E1A/RAS cells and assessed cell death following cisplatin treatment. As predicted from published data (31), silencing of PIN1 reduced cell death by the S47 variant, thus supporting a role for PIN1 in this cell death pathway **(Supp. Fig. 4A)**. Additionally, we found that silencing PIN1 markedly reduced the ability of the S47 variant to localize to the mitochondria, as assessed by PLA of S47 with TOMM20, which binds to mitochondrial p53 (33,34) (**Fig. 4D**).

A key step in the mitochondrial cell death pathway by p53 involves interaction with pro-apoptotic BAK; p53 induces conformational changes in BAK, leading to BAK oligomerization, cytochrome c release, and caspase activation (35). Whereas our data indicate that S47 traffics efficiently to mitochondria and binds to BAK, it remained formally possible that this variant was impaired for the ability to drive BAK oligomerization. To address this, we performed BAK oligomerization assays using purified mitochondria and bacterially-expressed and purified WT and S47 proteins, isolated using either GST or 6-Histidine tags. Incubation of purified mitochondria with either GST-WT p53 or GST-S47 followed by incubation with the cross-linking agent BMH and SDS-PAGE led to the appearance of oligomerized BAK (76 kDa band, **Fig. 5**). Notably, S47 protein could induce BAK oligomerization in these assays slightly

better than WT p53, purified with either tag (**Fig. 5**). These data support the conclusion that once at the mitochondria, S47 protein is capable of inducing BAK oligomerization and cell death via the mitochondrial pathway.

Tumors containing the S47 variant show an enhanced mitochondrial cell death program following cisplatin treatment

To confirm and extend our findings, we next sought to test the premise that S47 tumors from cisplatin-treated mice also show enhanced usage of the mitochondrial cell death pathway. To do this, we performed PLA assays on formalin-fixed tumor material from WT and S47 tumors following cisplatin treatment and monitored p53 localization at mitochondria by assessing its interaction with TOMM20 and BAK. Not surprisingly, in untreated tumors there was no evidence for complexes between p53 and TOMM20, or p53 and BAK. However, there were marked increases in p53-TOMM20 and p53-BAK complexes in S47 cisplatin-treated tumors, compared to WT (**Fig. 6A and B**; **Supp. Fig. 4B-D**). These data confirm that the S47 variant shows increased engagement of the mitochondrial pathway in E1A/RAS induced tumors.

DISCUSSION

Personalized medicine is a concept that has been gaining appreciation over the years, yet there are few examples of truly personalized medicine approaches for cancer. Children with non-functional SNPs in TPMT do not get treated with 6-mercaptopurine or 6-thioguanine, in order to prevent highly toxic side effects. Individuals with melanoma are sequenced for mutations in the BRAF gene before being treated with BRAF inhibitors. And women with breast cancer are analyzed for ER positivity and HER2 level before being treated with SERMs (selective estrogen receptor modifiers) or Herceptin. It is important to note that these cases are all relatively clear-cut: these compounds either work, or don't work, based upon the genetics of the individuals (TPMT) or the tumors (SERMs, BRAF inhibitors, Herceptin). What we are proposing here is slightly different: in the case of S47 individuals with cancer, general cytotoxic chemotherapeutic drugs are likely to show some efficacy, but cisplatin and BET inhibitors should work better. This improved efficacy could have dramatic consequences on cancer survival in S47 individuals; greater efficacy means fewer treatments, and this leads to reduced chance that drug-resistant cells can emerge. We posit that African-descent individuals diagnosed with tumors where cisplatin is one therapeutic possibility (such as for example lung cancer, bladder cancer, or triple negative breast cancer) should be encouraged to undergo genotyping for the S47 SNP; we propose that S47 positive individuals should be treated with cisplatin or a BRD inhibitor, where the choice is a possibility.

Since its discovery in 1979, p53 has been a cornerstone of cancer biology, and mutational inactivation of this tumor suppressor is a hallmark of human cancer (36-38). Our group and others have obtained data that in addition to mutations, SNPs in p53 and p53-pathway genes can impact the signaling potential of this pathway, and likewise can adversely

impact cancer risk and therapy. We modeled the S47 SNP in mice and showed that S47 mice have high propensity for developing spontaneous liver and other cancers (13). One question remaining from our study was whether S47 was a poorer tumor suppressor in other cell types; here-in we show that this is the case. It remains to be determined why this is the case. One possibility is that the ferroptotic defect in S47 mice leads to significant iron accumulation in these cells (J. Leu, unpublished data). It is well-known that iron is required for cell proliferation because it is required for ribonucleotide reductase and other enzymes in cell division (39,40). This may explain the increase in Ki-67 staining in S47 tumors compared to WT.

It is well established that p53 can promote apoptosis using a variety of different mechanisms (41,42). While the canonical role of p53 as a transcriptional activator of pro-apoptotic genes is well characterized, it is also clear that p53 possesses a transcription-independent role in apoptosis, by binding to BCL2 family members (9,43). Multiple reports have shown that this occurs in part by the ability to p53 to traffic to the mitochondria of transformed cells, in turn causing the oligomerization of the pro-apoptotic effectors BAK and BAX, leading to cytochrome c release and caspase activation (9-11). We found that S47 transformed MEFs, which are more sensitive to cisplatin, show increased trafficking of p53 to the mitochondria and increased ability to oligomerize BAK, suggesting that S47 cells show enhanced apoptosis by activating the mitochondrial cell death program. We also show that PIN1, which is required for mitochondrial localization of p53 (31), shows enhanced binding to S47 protein, thus providing a mechanistic explanation for our findings (see model **Fig. 6C**). Some of these findings were quite surprising, given that phosphorylated serine 46 is a major docking site for PIN1 (31). However, PIN1 binding to p53 occurs on several other phosphorylated residues (32); additionally, other post-translational modifications on p53 are

implicated in mitochondrial trafficking (44,45). One possibility is that serine 47 is a site for phosphorylation by casein kinase II, and this may influence mitochondrial trafficking or cell death by p53. We have been unable to detect the phospho-S47 species in human or mouse cells using polyclonal antisera raised against this phosphopeptide (M. Murphy, unpublished results); however we cannot rule out this formal possibility.

We find that S47 protein can directly cause BAK oligomerization; these data contrast with the findings of Kriwacki and colleagues, who show that the S47 variant of p53 cannot oligomerize BAX (46). While the results of that study indicate that the S47 variant might be impaired for certain aspects of the mitochondrial pathway, we clearly find that this is not the case. The reasons for this discrepancy are unclear: it could reflect the pro-apoptotic target protein analyzed in our study versus theirs (BAK versus BAX), the form of p53 used (they used an N terminal fragment of p53 while we used full length) or other assay-specific differences. We were unable to detect a p53-BAX complex or oligomerized BAX in our cells so we were unable to address this discrepancy directly.

Our data indicate that cisplatin, but not several other DNA damaging agents tested, preferentially induces the mitochondrial pathway of p53-mediated apoptosis. The reasons for this activity of cisplatin are unclear, but our data are consistent with the findings of others. Cisplatin is known to use the protein TAB1 to activate p38α, which activates p53 to engage the direct mitochondrial pathway of cell death (47). Additionally, cisplatin-mediated apoptosis requires p53-mediated generation of reactive oxygen species (ROS); ROS then facilitates mitochondrial localization of p53 (48). We consistently find that the ROS levels of S47 cells are higher than WT cells (S. Basu, unpublished data). Finally, unlike most other genotoxic

agents, cisplatin forms a variety of structural adducts on DNA that inhibit transcription, thus dampening the p53-dependent transcriptional pathway (49,50). These combined factors likely explain the preferential use of the direct mitochondrial pathway of cell death by S47 in response to cisplatin.

Collectively, our data suggest that personalized medicine approaches to chemotherapy based upon a p53 SNP are possible and promising. It is important to note that while we see increased cytotoxicity by cisplatin in transformed S47 cells, we see the opposite for non-transformed S47 cells and tissues, which show reduced cytotoxicity by cisplatin, compared to cells or tissues with WT p53 (13). These data augur well for the use of cisplatin in S47 individuals with cancer. It is our hope that this research will spur the genotyping of African Americans with cancer, in order to improve the therapeutic success and survival of these individuals.

ACKNOWLEDGMENTS

This work was supported by R01 CA201430 (M.E. Murphy), R01 CA102184 (M.E. Murphy.), R01 CA139319 (M.E. Murphy, D.L. George and J.I. Leu), P01 CA114046 (M.E. Murphy, D.L. George and J.I. Leu), TL1TR002344 (C.P. Kung) and F32 CA220972 (T. Barnoud). The Molecular Pathology and Imaging Core at Penn is funded by the Center for Molecular Studies in Digestive and Liver Diseases (NIH P30 DK050306), P01 CA098101 and P01 DK049210. Support for the Core Facilities used in this study was provided by Cancer Center Support Grant CA010815 to The Wistar Institute. The authors would like to acknowledge the Histotechnology, Laboratory Animal, Molecular Screening and Imaging facilities at The Wistar Institute. The authors would also like to thank Joshua Parris and Keerthana Gnanapradeepan in the Murphy lab for assistance and thoughtful discussions, and Ileabett Echeverria-Vargas for help with administration of OTX-015.

REFERENCES

1. Horn HF, Vousden KH. Coping with stress: multiple ways to activate p53. Oncogene 2007;26(9):1306-16.
2. Vousden KH, Ryan KM. p53 and metabolism. Nat Rev Cancer 2009;9(10):691-700.
3. Vousden KH, Prives C. Blinded by the Light: The Growing Complexity of p53. Cell 2009;137(3):413-31.
4. Zilfou JT, Lowe SW. Tumor suppressive functions of p53. Cold Spring Harb Perspect Biol 2009;1(5):a001883.
5. Stockwell BR, Friedmann Angeli JP, Bayir H, Bush AI, Conrad M, Dixon SJ, et al. Ferroptosis: A Regulated Cell Death Nexus Linking Metabolism, Redox Biology, and Disease. Cell 2017;171(2):273-85.
6. Gnanapradeepan K, Basu S, Barnoud T, Budina-Kolomets A, Kung C-P, Murphy ME. The p53 Tumor Suppressor in the Control of Metabolism and Ferroptosis. Frontiers in Endocrinology 2018;9(124).
7. Lowe SW, Bodis S, McClatchey A, Remington L, Ruley HE, Fisher DE, et al. p53 status and the efficacy of cancer therapy in vivo. Science 1994;266(5186):807-10.
8. Sullivan A, Syed N, Gasco M, Bergamaschi D, Trigiante G, Attard M, et al. Polymorphism in wild-type p53 modulates response to chemotherapy in vitro and in vivo. Oncogene 2004;23(19):3328-37.
9. Mihara M, Erster S, Zaika A, Petrenko O, Chittenden T, Pancoska P, et al. p53 has a direct apoptogenic role at the mitochondria. Mol Cell 2003;11(3):577-90.
10. Chipuk JE, Kuwana T, Bouchier-Hayes L, Droin NM, Newmeyer DD, Schuler M, et al. Direct activation of Bax by p53 mediates mitochondrial membrane permeabilization and apoptosis. Science 2004;303(5660):1010-4.
11. Leu JI, Dumont P, Hafey M, Murphy ME, George DL. Mitochondrial p53 activates Bak and causes disruption of a Bak-Mcl1 complex. Nat Cell Biol 2004;6(5):443-50.
12. Murphy ME, Liu S, Yao S, Huo D, Liu Q, Dolfi SC, et al. A functionally significant SNP in TP53 and breast cancer risk in African-American women. NPJ Breast Cancer 2017;3:5.
13. Jennis M, Kung CP, Basu S, Budina-Kolomets A, Leu JI, Khaku S, et al. An African-specific polymorphism in the TP53 gene impairs p53 tumor suppressor function in a mouse model. Genes Dev 2016;30(8):918-30.
14. Li X, Dumont P, Della Pietra A, Shetler C, Murphy ME. The codon 47 polymorphism in p53 is functionally significant. J Biol Chem 2005;280(25):24245-51.
15. Basu S, Barnoud T, Kung CP, Reiss M, Murphy ME. The African-specific S47 polymorphism of p53 alters chemosensitivity. Cell Cycle 2016;15(19):2557-60.
16. Feoktistova M, Geserick P, Leverkus M. Crystal Violet Assay for Determining Viability of Cultured Cells. Cold Spring Harb Protoc 2016;2016(4):pdb prot087379.
17. Franken NA, Rodermond HM, Stap J, Haveman J, van Bree C. Clonogenic assay of cells in vitro. Nat Protoc 2006;1(5):2315-9.
18. Pietsch EC, Perchiniak E, Canutescu AA, Wang G, Dunbrack RL, Murphy ME. Oligomerization of BAK by p53 utilizes conserved residues of the p53 DNA binding domain. J Biol Chem 2008;283(30):21294-304.
19. Basu S, Gnanapradeepan K, Barnoud T, Kung CP, Tavecchio M, Scott J, et al. Mutant p53 controls tumor metabolism and metastasis by regulating PGC-1alpha. Genes Dev 2018;32(3-4):230-43.

20. Frank AK, Leu JI, Zhou Y, Devarajan K, Nedelko T, Klein-Szanto A, et al. The codon 72 polymorphism of p53 regulates interaction with NF-{kappa}B and transactivation of genes involved in immunity and inflammation. Mol Cell Biol 2011;31(6):1201-13.
21. Littell RC. SAS system for mixed models. Cary, N.C.: SAS Institute Inc.; 1996. xiv, 633 p. p.
22. Rothman K, Greenland, S. Modern Epidemiology, 2nd Edition. Philadelphia, PA: Lippincott Williams & Wilkins; 1998.
23. Filippakopoulos P, Qi J, Picaud S, Shen Y, Smith WB, Fedorov O, et al. Selective inhibition of BET bromodomains. Nature 2010;468(7327):1067-73.
24. Amorim S, Stathis A, Gleeson M, Iyengar S, Magarotto V, Leleu X, et al. Bromodomain inhibitor OTX015 in patients with lymphoma or multiple myeloma: a dose-escalation, open-label, pharmacokinetic, phase 1 study. Lancet Haematol 2016;3(4):e196-204.
25. Berthon C, Raffoux E, Thomas X, Vey N, Gomez-Roca C, Yee K, et al. Bromodomain inhibitor OTX015 in patients with acute leukaemia: a dose-escalation, phase 1 study. Lancet Haematol 2016;3(4):e186-95.
26. Fu LL, Tian M, Li X, Li JJ, Huang J, Ouyang L, et al. Inhibition of BET bromodomains as a therapeutic strategy for cancer drug discovery. Oncotarget 2015;6(8):5501-16.
27. Delmore JE, Issa GC, Lemieux ME, Rahl PB, Shi J, Jacobs HM, et al. BET bromodomain inhibition as a therapeutic strategy to target c-Myc. Cell 2011;146(6):904-17.
28. Mertz JA, Conery AR, Bryant BM, Sandy P, Balasubramanian S, Mele DA, et al. Targeting MYC dependence in cancer by inhibiting BET bromodomains. Proc Natl Acad Sci U S A 2011;108(40):16669-74.
29. Leonetti C, Biroccio A, Candiloro A, Citro G, Fornari C, Mottolese M, et al. Increase of cisplatin sensitivity by c-myc antisense oligodeoxynucleotides in a human metastatic melanoma inherently resistant to cisplatin. Clin Cancer Res 1999;5(9):2588-95.
30. Schneider-Poetsch T, Ju J, Eyler DE, Dang Y, Bhat S, Merrick WC, et al. Inhibition of eukaryotic translation elongation by cycloheximide and lactimidomycin. Nat Chem Biol 2010;6(3):209-17.
31. Sorrentino G, Mioni M, Giorgi C, Ruggeri N, Pinton P, Moll U, et al. The prolyl-isomerase Pin1 activates the mitochondrial death program of p53. Cell Death Differ 2013;20(2):198-208.
32. Polonio-Vallon T, Kruger D, Hofmann TG. ShaPINg Cell Fate Upon DNA Damage: Role of Pin1 Isomerase in DNA Damage-Induced Cell Death and Repair. Front Oncol 2014;4:148.
33. Dumont P, Leu JI, Della Pietra AC, 3rd, George DL, Murphy M. The codon 72 polymorphic variants of p53 have markedly different apoptotic potential. Nat Genet 2003;33(3):357-65.
34. Park JH, Zhuang J, Li J, Hwang PM. p53 as guardian of the mitochondrial genome. FEBS Lett 2016;590(7):924-34.
35. Vaseva AV, Moll UM. The mitochondrial p53 pathway. Biochim Biophys Acta 2009;1787(5):414-20.
36. Hollstein M, Sidransky D, Vogelstein B, Harris CC. p53 mutations in human cancers. Science 1991;253(5015):49-53.
37. Petitjean A, Achatz MI, Borresen-Dale AL, Hainaut P, Olivier M. TP53 mutations in human cancers: functional selection and impact on cancer prognosis and outcomes. Oncogene 2007;26(15):2157-65.
38. Whibley C, Pharoah PD, Hollstein M. p53 polymorphisms: cancer implications. Nat Rev Cancer 2009;9(2):95-107.

39. Hoffbrand AV, Ganeshaguru K, Hooton JW, Tattersall MH. Effect of iron deficiency and desferrioxamine on DNA synthesis in human cells. Br J Haematol 1976;33(4):517-26.
40. Le NT, Richardson DR. The role of iron in cell cycle progression and the proliferation of neoplastic cells. Biochim Biophys Acta 2002;1603(1):31-46.
41. Bates S, Vousden KH. Mechanisms of p53-mediated apoptosis. Cell Mol Life Sci 1999;55(1):28-37.
42. Speidel D. Transcription-independent p53 apoptosis: an alternative route to death. Trends Cell Biol 2010;20(1):14-24.
43. Moll UM, Wolff S, Speidel D, Deppert W. Transcription-independent pro-apoptotic functions of p53. Curr Opin Cell Biol 2005;17(6):631-6.
44. Castrogiovanni C, Waterschoot B, De Backer O, Dumont P. Serine 392 phosphorylation modulates p53 mitochondrial translocation and transcription-independent apoptosis. Cell Death Differ 2018;25(1):190-203.
45. Nemajerova A, Erster S, Moll UM. The post-translational phosphorylation and acetylation modification profile is not the determining factor in targeting endogenous stress-induced p53 to mitochondria. Cell Death Differ 2005;12(2):197-200.
46. Follis AV, Llambi F, Merritt P, Chipuk JE, Green DR, Kriwacki RW. Pin1-Induced Proline Isomerization in Cytosolic p53 Mediates BAX Activation and Apoptosis. Mol Cell 2015;59(4):677-84.
47. Zhu Y, Regunath K, Jacq X, Prives C. Cisplatin causes cell death via TAB1 regulation of p53/MDM2/MDMX circuitry. Genes Dev 2013;27(16):1739-51.
48. Bragado P, Armesilla A, Silva A, Porras A. Apoptosis by cisplatin requires p53 mediated p38alpha MAPK activation through ROS generation. Apoptosis 2007;12(9):1733-42.
49. Todd RC, Lippard SJ. Inhibition of transcription by platinum antitumor compounds. Metallomics 2009;1(4):280-91.
50. Leu JI, George DL. Hepatic IGFBP1 is a prosurvival factor that binds to BAK, protects the liver from apoptosis, and antagonizes the proapoptotic actions of p53 at mitochondria. Genes Dev 2007;21(23):3095-109.

Figure Legends

Figure 1. S47 is an intrinsically poorer tumor suppressor.

(A, B) WT and S47 E1A/RAS MEFs were plated at a density of 20,000 cells per well in a 6-well plate under normal (A) or low serum (B) conditions and were counted daily for six days (n.s., not significant). * $p<0.05$

(C) WT and S47 E1A/RAS MEFs were plated in soft agar at a concentration of 8,000 cells per 60-mm dish and were incubated for 14 days (scale bar, 250 μm).

(D) Quantification of (C) both by colony number and colony size, as measured by the area of colonies using the equation $A=\pi r^2$. Colony number quantification was performed by counting the number of colonies in five random fields of view, and colony size was performed by quantifying the area of ten random colonies per group. *** $p<0.001$

(E) $1x10^6$ WT or S47 E1A/RAS MEFs were injected subcutaneously into the right flanks of 8-week old NSG mice. Tumors were measured using a digital caliper and tumor volumes were derived from the equation $v = (\text{length} \times \text{width}^2)/0.52$, where the width was the shortest of the two sides (n=10 mice per group). Each experiment is representative of two independent clones of each genotype.

(F) Measurements of the weights of WT and S47 E1A/RAS tumors taken at day 19. *** $p<0.001$

(G) IHC analysis of Ki-67 and p53 staining of WT and S47 E1A/RAS tumors (n=4 mice per group; scale bar, 100 μm). Rabbit IgG was used as a negative control.

Figure 2. S47 transformed MEFs show increased sensitivity to cisplatin and BET inhibitors but not etoposide.

(A) WT or S47 E1A/RAS cells were plated at a density of 10,000 cells per well in 24-well plates. The next day, cells were treated with the indicated concentrations of cisplatin (CDDP) for 72 hours. Cells were then fixed with 10% formalin and stained with 0.5% crystal violet. * $p<0.05$

(B) WT and S47 E1A/RAS cells were pre-treated with sub-lethal concentrations of CDDP (0.5 μM) or Etoposide (0.02 μM) for 24 hours and were then plated in soft agar in the absence of drug for 14 days (scale bar, 1000 μm).

(C) Quantification of (B).

(D) WT and S47 E1A/RAS cells were plated at a density of 2,000 cells per well in a 96-well plate. The next day, cells were treated with the indicated doses of Nedaplatin or Carboplatin for 72 hours and subjected to Alamar Blue assays.

(E) WT and S47 E1A/RAS cells were plated at a density of 1,000 cells per well in a 96-well plate. The next day, cells were treated with the indicated doses of the BET inhibitors JQ-1 or OTX-015 for 96 hours. Cells were then subjected to IC_{50} Alamar Blue assays.

(F) Colony formation assays of WT and S47 E1A/RAS cells that were treated with 10 μM OTX-015 for 24 hours prior to plating. Data are indicative of representative images of experiments done in triplicate and were performed on two independent clones of each genotype.

(G) Quantification of (E). *** $p<0.001$

Figure 3. Cisplatin and OTX-015 show superior efficacy in S47 tumors.

(A) $5x10^5$ WT and S47 E1A/RAS MEFs were injected subcutaneously into the right flanks of 7-8-week-old NSG mice. Once tumors reached an approximate size of 100 mm^3, mice were randomized into three groups (n=8 mice per group): (1) vehicle, (2) CDDP (4 mg/kg, every four days), and (3) OTX-015 (50 mg/kg, daily). Tumor volumes were measured every other day as previously described. Note the different scales for tumor volume between WT and S47. * = $p<0.05$, ** = $p<0.01$, and *** $p < 0.001$.

(B) Tumor weights of WT and S47 tumors treated with either CDDP or OTX-015.

(C) WT and S47 E1A/RAS MEFs were injected subcutaneously as in (A) to compare treatment efficacy between CDDP (4 mg/kg, every four days) and Etoposide (10 mg/kg, every four days).

(D) Tumor weights of WT and S47 tumors treated with either CDDP or Etoposide. Etoposide did not cause a statistically significant decrease in tumor growth compared to control.

(E-G) A mixed model with spline linear regression analysis showing that cisplatin and OTX-015, but not etoposide, caused significantly greater reduction in tumor volume per treatment in S47 tumors compared to WT.

(H) IHC analysis of Ki-67, Cleaved Caspase-3, and p53 staining of WT and S47 E1A/RAS tumors +/- CDDP (scale bar, 100 μm). Rabbit IgG was used as a negative control.

Figure 4. S47 tumor cells show increased utilization of the mitochondrial cell death pathway.

(A) WT and S47 E1A/RAS cells were treated with 10 μM CDDP for 24 hours in the presence or absence of the protein synthesis inhibitor cycloheximide (CHX, 2.5 μg/mL). Cell lysates were subjected to Western blot analysis, and immunoblotted for cleaved caspase-3, p53, p21, and HSP90 (loading control). CDDP: cisplatin

(B) WT and S47 E1A/RAS cells were treated with 10 μM cisplatin (CDDP) for 24 hours. Cells were then fractionated into three fractions: whole cell lysate (W), mitochondria (M), and cytosol (C). Equal μg of lysates were probed for the mitochondrial protein BAK and cytochrome c (cyto c) and the nuclear/cytosolic protein PCNA to assess purity. Arrows depict p53 protein levels in mitochondrial fractions of WT vs. S47 cells treated with CDDP. Increased localization of S47 protein to mitochondria was evident in multiple independent experiments, including those where the levels of total WT p53 and S47 were closely matched.

(C) An in-situ proximity ligation assay (PLA) was performed in WT and S47 E1A/RAS cells treated with 10 μM CDDP for 12 hours. Each red dot represents interaction between endogenous p53 and PIN1 proteins (scale bar, 25 μm). Cells stained with p53 antibody alone were used as a negative control. DAPI nuclear staining is shown in blue. The white boxed image is magnified in the panel to the right. Shown on the right is the quantification of (C), measured as the average number of PLA signals per nuclei. Data was quantitated by counting the number of cells in five random fields of view per experimental group. CDDP: cisplatin. * $p<0.05$ and *** $p<0.001$

(D) S47 E1A/RAS cells were transfected with si-PIN1 for 48 hours. Cells were then treated with 10 μM CDDP for 12 hours and were subjected to an in-situ PLA assay. Each red dot

represents interaction between endogenous p53 and TOMM20 proteins (scale bar, 25 μm). Cells stained with p53 antibody alone were used as a negative control. Shown on the right are Western blot analyses showing efficient knockdown of PIN1, as well as similar expression of p53 and TOMM20 in si-ctr and si-PIN1 S47 E1A/RAS cells. ** $p<0.01$

Figure 5. The S47 variant of p53 shows increased ability to oligomerize BAK.

Equal amounts of whole cell (WCE), cytosolic (Cyto) and mitochondrial (Mito) extracts prepared from p53-null human H1299 cells were immunoblotted for mitochondrial protein BAK and the nuclear-cytoplasmic protein PCNA (left). Purified mitochondria (25 µg) were incubated with 100 pmol of full-length (FL) GST-p53 (middle panel) or His-tagged p53 (right panel) recombinant proteins, as indicated. The asterisk in the His-tagged panel reflects a likely degradation product. BAK oligomers were crosslinked with BMH, resolved by SDS-PAGE and detected by Western blotting with a BAK−specific antibody (anti BAK NT). The BAK oligomerization blots were reprobed with an antibody against p53 to verify equal quantity and purity of added p53 recombinant proteins used in the BAK activation assays, as indicated.

Figure 6. Increased mitochondrial trafficking of S47 protein in tumors.

(A) Detection of p53 and TOMM20 interactions in Formalin Fixed Paraffin Embedded (FFPE) WT and S47 E1A/RAS tumors using the Duolink PLA Brightfield kit. Staining without primary antibodies was used as a negative control. PLA signals are shown as reddish-brown dots, indicated by black arrowheads (scale bar, 20 μm).

(B) Quantification of p53-TOMM20 PLA of WT and S47 tumors +/- CDDP. S47 tumors treated with CDDP show a significantly greater number of PLA-positive dots compared to WT treated tumors. Quantification was performed by counting the number of PLA positive signals in five random fields of view for each experimental group, each done in triplicate.

(C) Proposed model highlighting the increased usage of the direct mitochondrial pathway of p53-mediated cell death in S47 tumors treated with cisplatin.

Author Manuscript Published OnlineFirst on August 16, 2018; DOI: 10.1158/0008-5472.CAN-18-1327
Author manuscripts have been peer reviewed and accepted for publication but have not yet been edited.

Figure 1

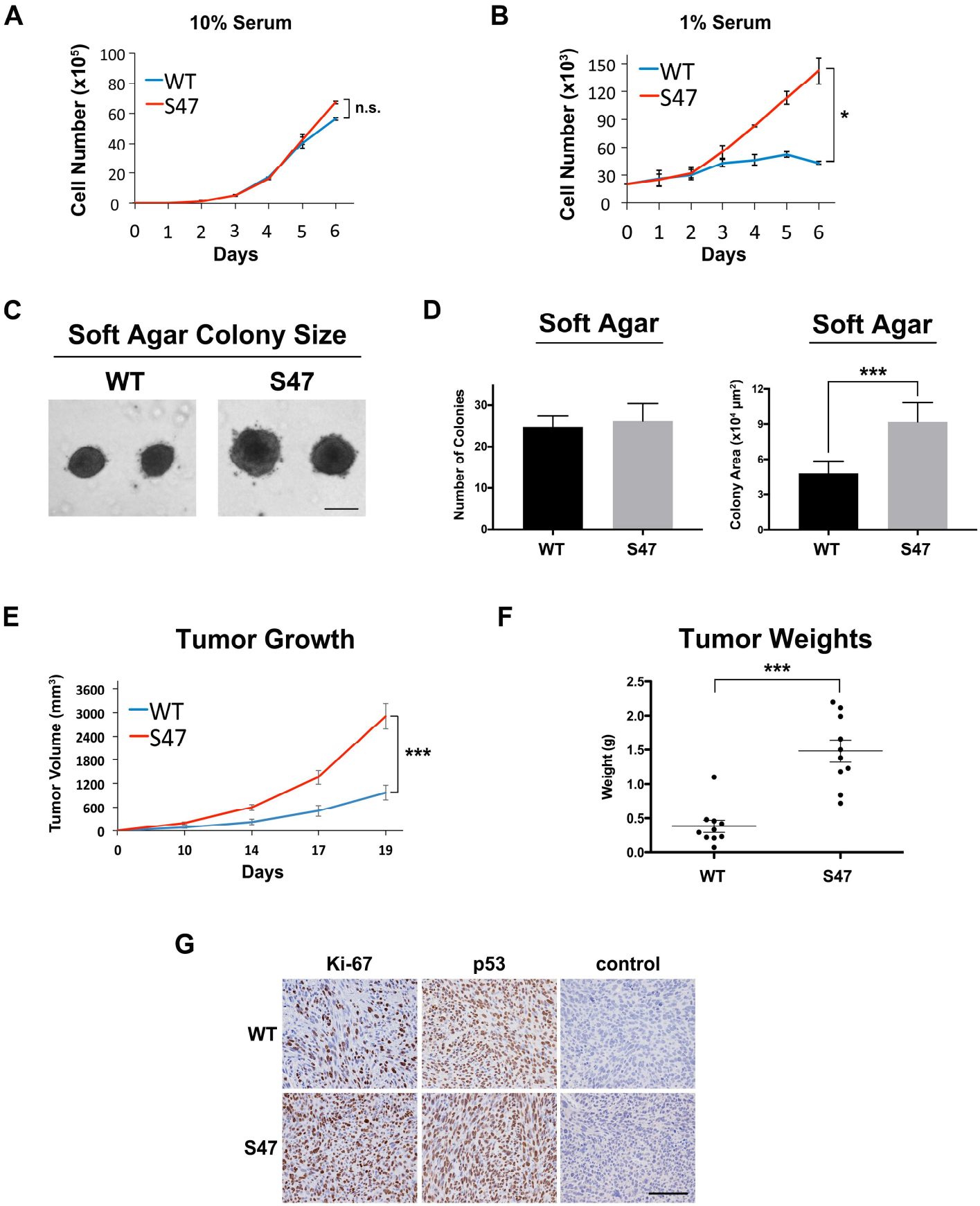

Author Manuscript Published OnlineFirst on August 16, 2018; DOI: 10.1158/0008-5472.CAN-18-1327
Author manuscripts have been peer reviewed and accepted for publication but have not yet been edited.

Figure 2

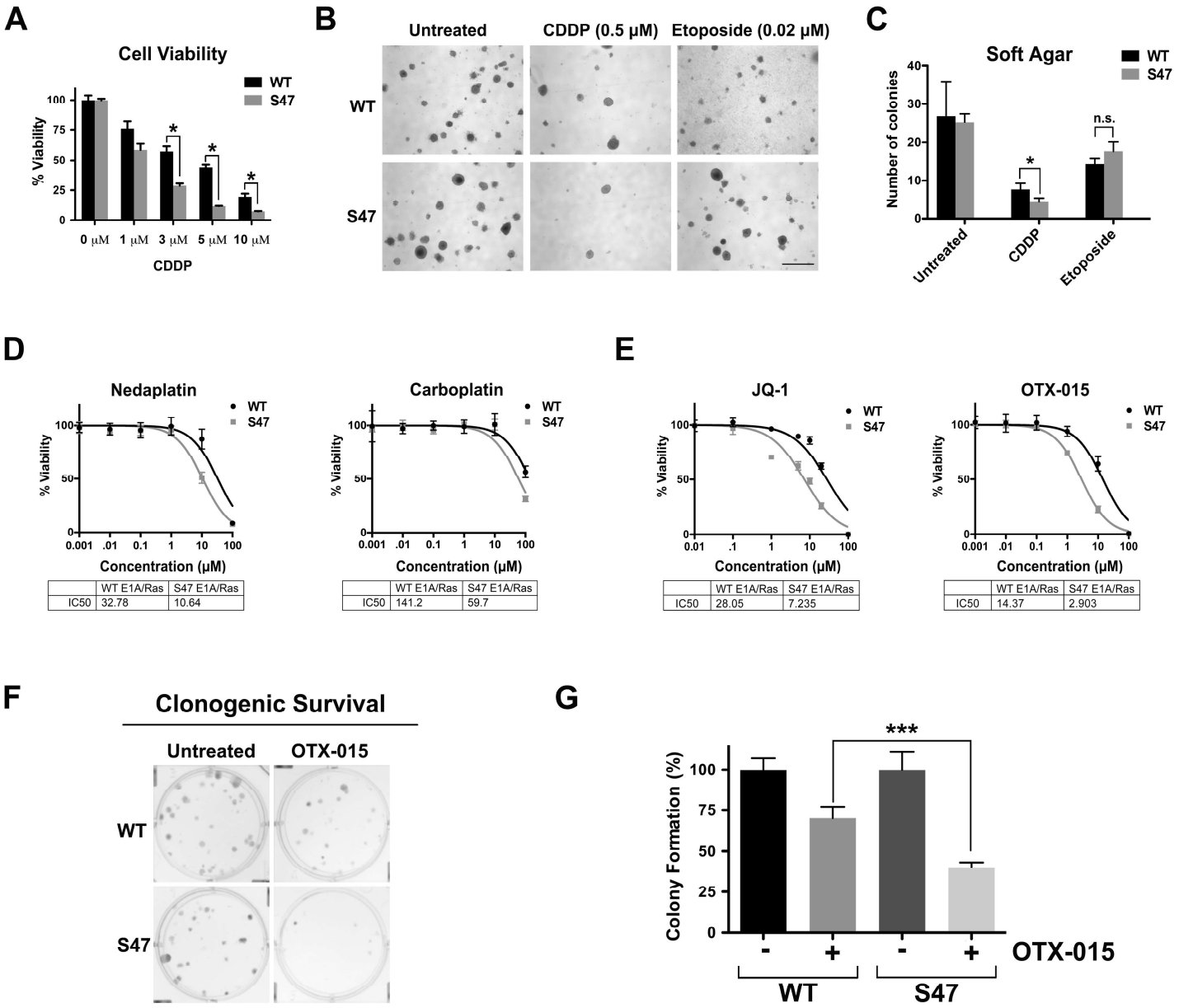

D	WT E1A/Ras	S47 E1A/Ras
IC50	32.78	10.64

D	WT E1A/Ras	S47 E1A/Ras
IC50	141.2	59.7

E	WT E1A/Ras	S47 E1A/Ras
IC50	28.05	7.235

E	WT E1A/Ras	S47 E1A/Ras
IC50	14.37	2.903

Author Manuscript Published OnlineFirst on August 16, 2018; DOI: 10.1158/0008-5472.CAN-18-1327
Author manuscripts have been peer reviewed and accepted for publication but have not yet been edited.

Figure 3

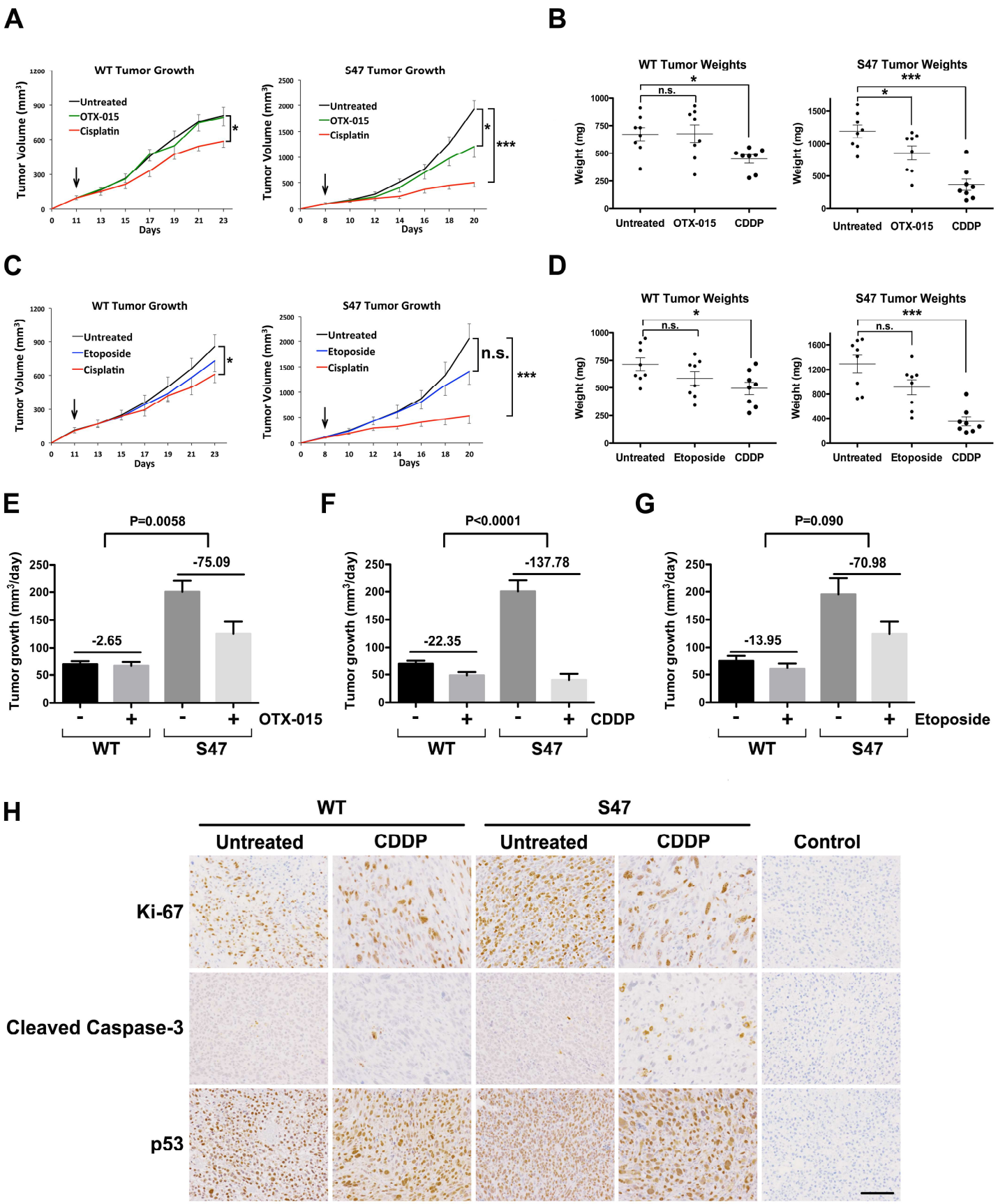

Author Manuscript Published OnlineFirst on August 16, 2018; DOI: 10.1158/0008-5472.CAN-18-1327
Author manuscripts have been peer reviewed and accepted for publication but have not yet been edited.

Figure 4

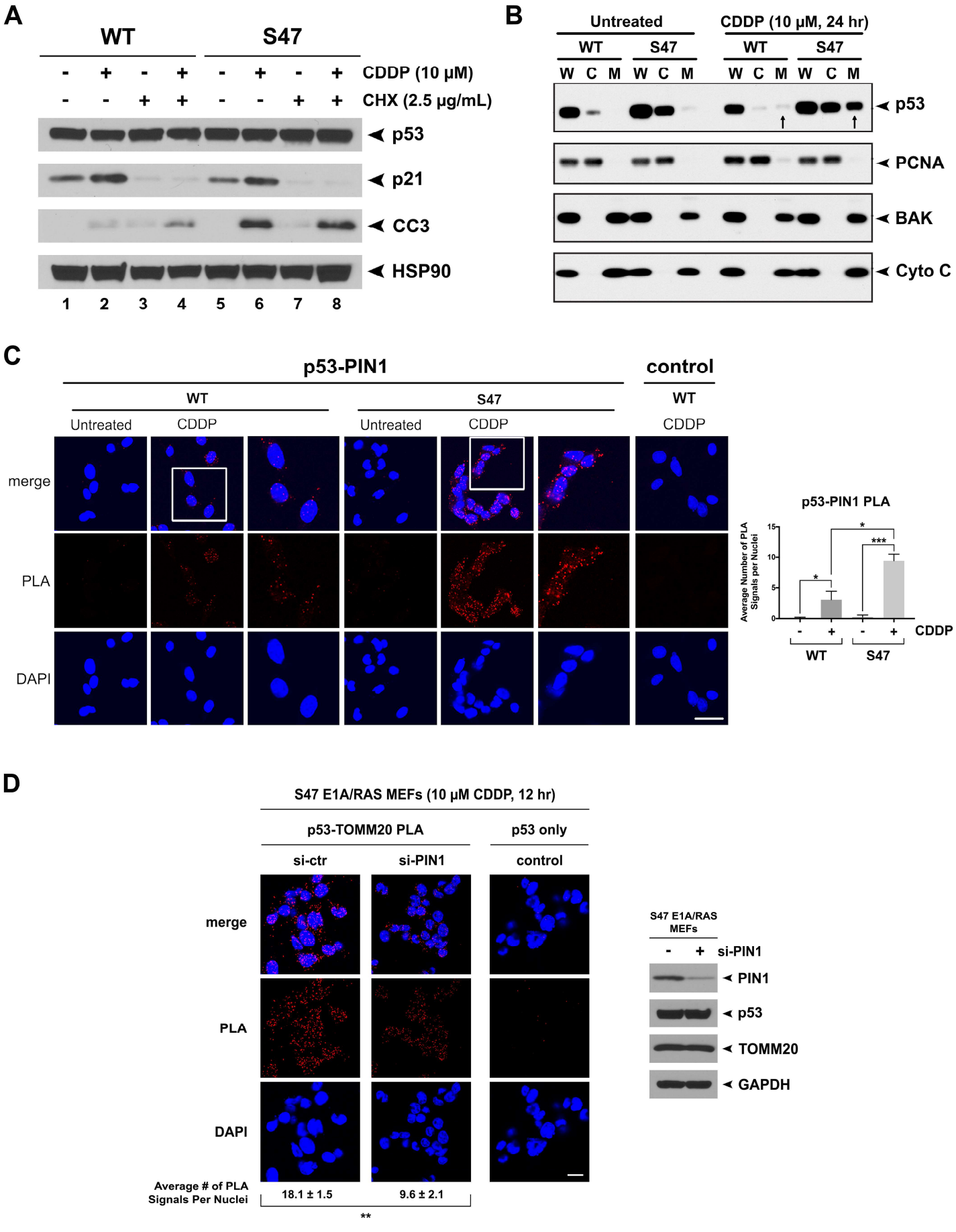

Figure 5

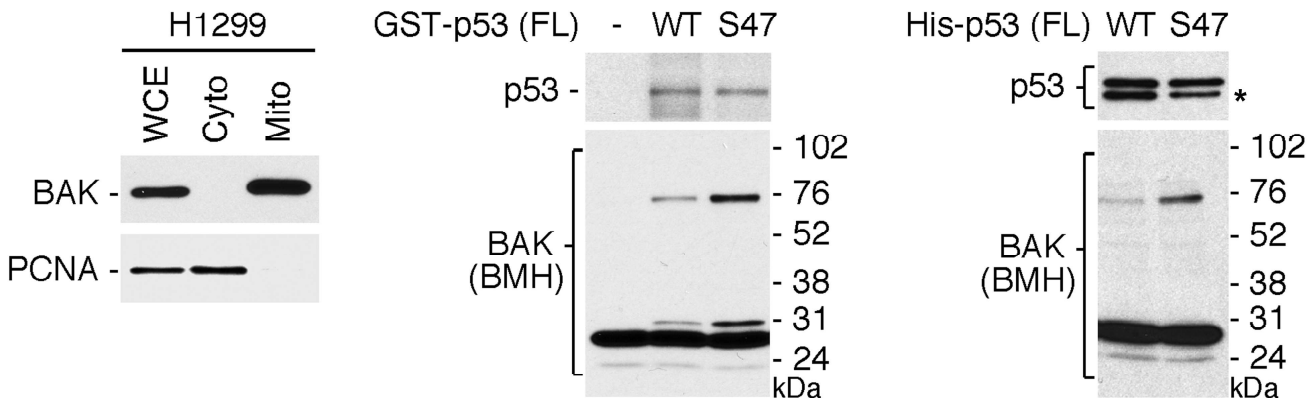

Author Manuscript Published OnlineFirst on August 16, 2018; DOI: 10.1158/0008-5472.CAN-18-1327
Author manuscripts have been peer reviewed and accepted for publication but have not yet been edited.

Figure 6

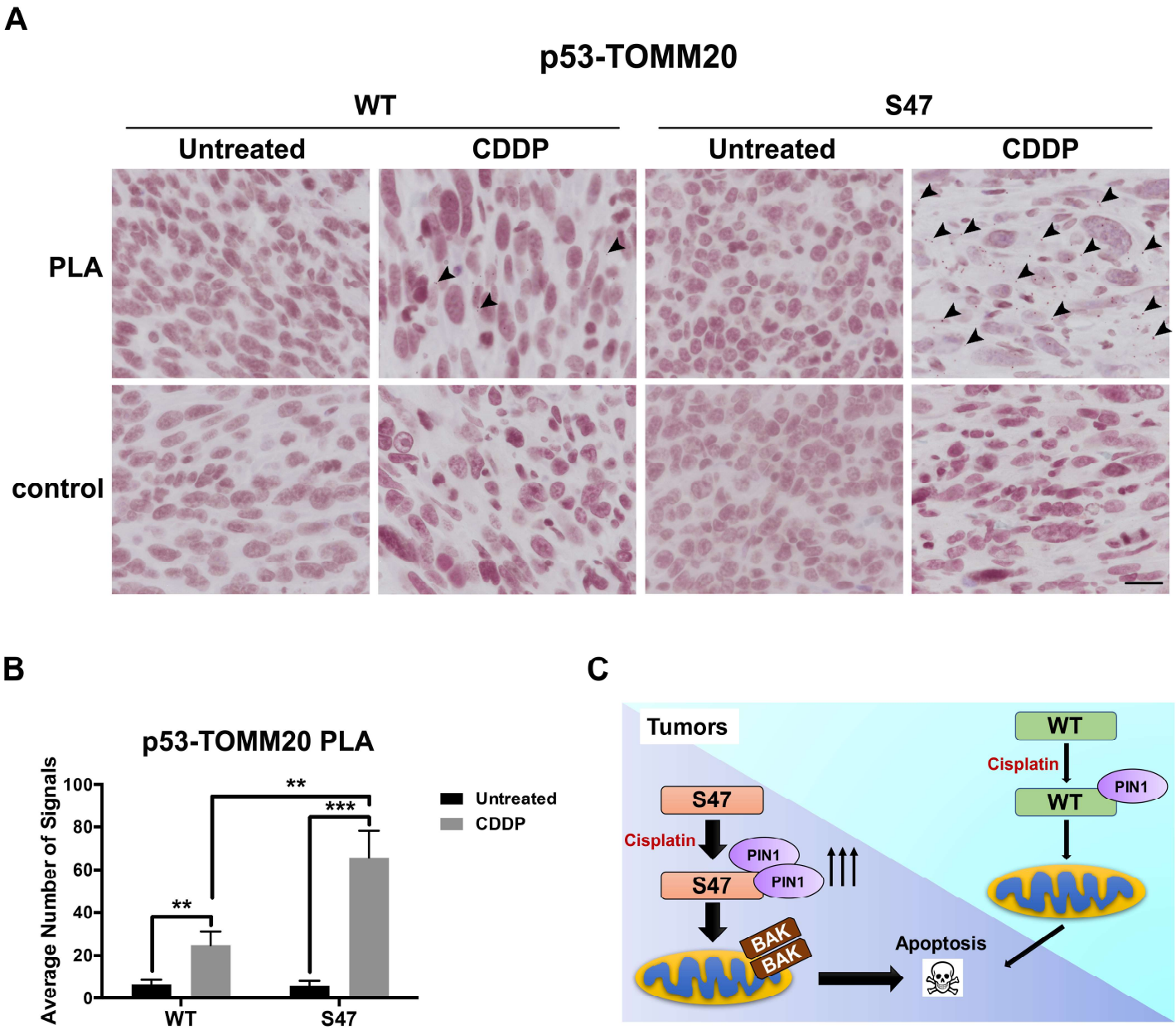

AACR American Association for Cancer Research

Cancer Research

The Journal of Cancer Research (1916–1930) | The American Journal of Cancer (1931–1940)

Tailoring chemotherapy for the African-centric S47 variant of TP53

Thibaut Barnoud, Anna Budina-Kolomets, Subhasree Basu, et al.

Cancer Res Published OnlineFirst August 16, 2018.